Effects of topological solitons on autocorrelation functions for chains of coupled torsional oscillators

Dennis Perchak, Robert Yaris, and Jeffrey Skolnick

Department of Chemistry, Washington University, St. Louis, Missouri 63130
(Received 15 November 1982; accepted 16 February 1983)

Brownian dynamics computer simulations were performed on chains of coupled torsional oscillators. The purpose was to observe the changes in autocorrelation functions, related to typical experimental measurements, caused by the introduction of topological solitons or kinks into the system. We considered three model systems: a chain of coupled torsional oscillators, a chain of coupled torsional oscillators with additional onefold rotational potentials acting on each oscillator, and a chain of coupled torsional oscillators with additional threefold rotational potentials. These models are of interest because of their application to torsional motions in polymeric systems, and, in particular, the system with onefold rotational potentials has been studied extensively as the sine–Gordon chain. We present simulation results for three autocorrelation functions of these three systems both with and without topological solitons.

I. INTRODUCTION

The concepts of solitons or kinks have been applied to numerous physical systems in recent years. Examples include dislocations in crystals,[1,2] domain walls in ferromagnets,[3] electron mobility in polyacetylene,[4,5] localized defects in crystalline polyethylene,[6,7] in particle physics,[8] and many others.[9] As solitons or kinks are proffered as the dominant mechanism for an ever increasing variety of physical systems, one is led to ask a rather simple and fundamental question. That is, what differences are there in typical experimental measurements between a system that contains a soliton (or solitons) and the same system without any solitons? It is our intention to study some examples of this question through the use of computer simulations.

Solitons can occur in a physical system in two different ways. They can occur due to the equation of motion of the system since if the system has a nonlinear equation of motion it can lead to solitonlike solutions. These soliton states can then be thermally populated just as any other states are. Solitons arising due to the equation of motion (or dynamics of the system) are sometimes referred to as dynamic solitons. Solitons can also occur in a physical system due to the kinematics of the problem. An example of this is a localized defect. Such solitons are independent of the nature of the equation of motion, in fact are an initial condition, and are sometimes called topological solitons. Since they arise from an initial condition they must be explicitly introduced into a model for the system. Although we shall explicitly introduce the solitons into the models we consider, the type of solitons introduced are the same as would arise thermally in our models.

Brownian dynamics[10–13] allow us to simulate the system (e. g., a polymer chain) in contact with its surroundings (e. g., the solvent or other polymer chains) which is the physically realistic situation. In solving the dynamics of the chain on a computer we are limited to solving the problem for a finite chain. By using reentrant boundary conditions one makes the finite chain mimic the results of an infinite chain up to Fourier components having a wavelength greater than the length of the finite chain. Our procedure will be as follows: We will consider several model systems for which we can control the presence or absence of kinks. Using Brownian dynamics, we will simulate the motion of these systems with and without kinks. During the simulations, we will calculate (or measure) autocorrelation functions, from which one can obtain typical experimental quantities. A comparison between systems with kinks and those without will then be made.

The model systems we choose to study consist of a set of coupled torsional oscillators or beads that interact through nearest-neighbor torsional springs. We are interested only in torsional motion; thus each bead can only rotate not translate. In addition, each bead may be subjected to single-bead m-fold rotational potentials. In this paper we consider values of $m = 0$, 1, 3. With reentrant boundary conditions we introduce kinks or solitons into the system by placing a twist on the spring between the first and last oscillators; this forces the chain to support a phase difference along the chain. The advantage of placing kinks into the system in this fashion is that these kinks, once introduced, remain in the system and one thus knows exactly how many solitons the system has. The same kinks would occur as dynamic or thermal kinks in either an infinite or reentrant system of the type we are now modeling as kink–antikink pairs. (Strictly speaking this is not the case for $m = 0$, the absence of a rotational barrier, which does not support a true soliton since any twist will delocalize over the whole chain.) Such antipairs eventually annihilate and are thermally reformed. For the choice of parameters we use, the thermal density of kink–antikink pairs is of the order e^{-8}, hence we need not concern ourselves with them. If we wanted to study the effects of solitons at thermal equlibrium in our model we would have had to change the parameters we used drastically. We have taken the opposite approach and effectively eliminated the thermally generated solitons. In fact we have gone over to an unrealistically high density of kinks, one or two per 30 beads in an effort to observe their effects.

The above model systems are of interest because of

 0021-9606/83/116914-14$02.10

their use in modeling torsional motions in polymers[14,15] and torsion dynamics in DNA.[16,17] In particular the torsional oscillator system with a threefold barrier is a reasonable model for conformations of a polymer chain. It should be noted that these models are not models of real systems since obviously a real molecule goes into itself on a 2π twist (it does not have a spring). However, they are representative of the class of real toplogical solitons. Related one-dimensional polymer models have also been considered by Weiner and Pear,[13] Helfand,[12] and Cook and Livernese.[18] The system with additional onefold rotational barriers is known as the sine–Gordon chain[1,19–21] and has received a great deal of attention as it is the discretized version of the sine–Gordon equation which possesses dynamic soliton solutions.[9,6,22–24] The quantities that we wish to utilize in our comparison of soliton and nonsoliton systems are the velocity autocorrelation function and the first and second Legendre polynomial autocorrelation functions of the rotational dipole (the net change in torsional angle). These are quantities which typically can be related to measurements in light scattering, dielectric relaxation, fluorescence depolarization, or NMR relaxation experiments. It should be noted that all of these autocorrelation functions are measuring all the beads in the system. We have purposely not looked at measurements which are direct signatures of the solitons (such as the electron spin resonance of the unpaired electron in the soliton in polyacytelene) or at the changes in the eigenvalue spectrum introduced by the solitons. This was done since it is our object to investigate in what way such nonspecific measurements are changed by the presence of solitons.

The outline of this paper is as follows: In Sec. II, we describe in detail the model systems and the method of simulation. We also define the calculation of the correlation functions. In Sec. III, we present results of the computer simulations. We first test the simulation method by comparing results from the simulations with analytic solutions to the simplest of the model systems, the coupled torsional oscillator model lacking any additional rotational barriers. We then compare and contrast the various model systems for different values of the model parameters in the presence and the absence of kinks. A general summary and conclusion are presented in Sec. IV.

II. DESCRIPTION OF THE MODEL

The model consists of a chain of N beads that interact via nearest-neighbor torsional springs (with torsion constant K'). Only rotational motion of the beads is considered; thus the motion of the ith bead is given by an angular coordinate $\theta_i(t')$ and an angular velocity $\dot{\theta}_i(t')$. Reentrant boundary conditions are used; i. e., $\theta_{N+1}=\theta_1$. This enables one to obtain the effects of an infinite chain using only a relatively small number of beads. A kink or soliton can be introduced into the chain by placing a twist of magnitude δ on the spring connecting the first and Nth beads. A nonzero δ means that the chain must support a phase difference of δ from θ_1 to θ_N. Additionally, the beads can be subjected to single-particle m-fold rotational potentials of barrier height E_b'.

The Lagrangian for this system is

$$L=\sum_{i=1}^{N}\{\tfrac{1}{2}J\dot{\theta}_i^2-\tfrac{1}{2}E_b'[1-\cos(m\theta_i)]\}-\tfrac{1}{2}K'\sum_{i=1}^{N-1}(\theta_{i+1}-\theta_i)^2-\tfrac{1}{2}K'(\theta_1-\theta_N-\delta)^2\,, \tag{1}$$

where J is the moment of inertia for a bead. Since our interest lies in the dynamics of the chain in interaction with its surroundings, we regard the beads as being in contact with a heat bath of temperature T'. The resulting Langevin equations are

$$J\ddot{\theta}_1=K'(\theta_N+\theta_2+\delta-2\theta_1)-\tfrac{1}{2}mE_b'\sin(m\theta_1)-\beta'J\dot{\theta}_1+A_1'(t')\,; \tag{2a}$$

$$J\ddot{\theta}_i=K'(\theta_{i+1}+\theta_{i-1}-2\theta_i)-\tfrac{1}{2}mE_b'\sin(m\theta_i)-\beta'J\dot{\theta}_i+A_i'(t')\,,\quad 2\le i\le N-1\,; \tag{2b}$$

$$J\ddot{\theta}_N=K'(\theta_1+\theta_{N-1}-\delta-2\theta_N)-\tfrac{1}{2}mE_b'\sin(m\theta_N)-\beta'J\dot{\theta}_N+A_N'(t')\,. \tag{2c}$$

The effects of the heat bath are given by a phenomenological damping $-\beta'J\dot{\theta}_i$ and a random force (torque) on each bead $A_i'(t')$ with the statistical properties

$$\langle A_i'(t')\rangle=0\,,\qquad \langle A_i'(t_1')A_j'(t_2')\rangle=2J\beta'k_BT'\delta(t_1'-t_2')\delta_{ij}\,, \tag{3}$$

where k_B is Boltzmann's constant and the angular brackets denote ensemble averages.

For the computer simulation, it is more convenient to work in the dimensionless units

$$t=t'(k_BT_0'/J)^{1/2}\,,\quad K=K'/k_BT_0'\,,\quad T=T'/T_0'\,,\quad \beta=\beta'(J/k_BT_0')\,,\quad E_b=E_b'/k_BT_0'\,, \tag{4}$$

where T_0' is some reference temperature (note that J scales out of the equations on performing the coordinate transformation). The Langevin equations for the system then become

$$\ddot{\theta}_1=K(\theta_N+\theta_2+\delta-2\theta_1)-\tfrac{1}{2}mE_b\sin(m\theta_1)-\beta\dot{\theta}_1+A_1(t)\,; \tag{5a}$$

$$\ddot{\theta}_i=K(\theta_{i+1}+\theta_{i-1}-2\theta_i)-\tfrac{1}{2}mE_b\sin(m\theta_i)-\beta\dot{\theta}_i+A_i(t)\,,\quad 2\le i\le N-1\,; \tag{5b}$$

$$\ddot{\theta}_N=K(\theta_1+\theta_{N-1}-\delta-2\theta_N)-\tfrac{1}{2}mE_b\sin(m\theta_N)-\beta\dot{\theta}_N+A_N(t) \tag{5c}$$

and the random force terms are now given by

$$\langle A_i(t)\rangle=0\,,\quad \langle A_i(t_1)A_j(t_2)\rangle=2\beta T\delta(t_1-t_2)\delta_{ij}\,. \tag{6}$$

A Brownian dynamics simulation involves generating a statistically representative trajectory for the system defined by the Langevin Eqs. (5)–(6). The numerical procedure employed is due to Helfand[25] and consists of an extension of Runge–Kutta methods to stochastic differential equations such as the Langevin equation. We use Helfand's method to second order.

Depending on the parameters chosen, the Langevin equations (5) and (6) represent several, different model systems. We shall consider the following ones:

(1) $E_b=m=0$. This system consists of nearest-neighbor torsion coupled beads. There are no addition-

al, single-particle rotational potentials. We will refer to this system as a "no barrier" system.

(2) $m=3$. This system, possesses in addition to the torsional coupling between beads, a threefold single-particle rotational potential acting on each bead and models a homopolymer chain. This will be referred to as a "threefold barrier" system. We will consider threefold barrier systems with $E_b=2T$ and $E_b=3T$. (Note that at room temperature $3T\simeq 1.8$ kcal/mol, a representative value for a conformational barrier in polyethylene.)

(3) $m=1$. This system, the sine–Gordon chain, has in addition to the torsional potential, a onefold rotational potential acting on each bead and is called the "onefold barrier" system. Again, we consider both $E_b=2T$ and $E_b=3T$. We will investigate these three systems with $\delta=0$ (nonkinked systems) and their corresponding systems with $\delta\neq 0$ (kinked systems). We will consider values of $\delta=0$, 2π, or 4π. For all the above systems we will use the following values for the remaining parameters: $K=1$; $T=1$; $\beta=3$; $N=30$. If one considers a simple harmonic oscillator in a well of curvature $K=1$, then critical damping is given by $\beta=2$. In this sense, all our model systems are overdamped, which is typical for a polymer chain in solution (or in the solid).

Our primary goal in this work is to explore the manner in which the presence of topological kinks affects the dynamics of a system in relation to correlation functions that might be measured experimentally. To this end, we examine the above systems with and without kinks and compare the resulting correlation functions. The correlation functions we consider are:

$$V_\theta(\tau)=\frac{1}{N}\sum_{i=1}^{N}\langle\dot\theta_i(\tau)\dot\theta_i(0)\rangle\,, \tag{7a}$$

$$P_1(\tau)=\frac{1}{N}\sum_{i=1}^{N}\langle\cos[\theta_i(\tau)-\theta_i(0)]\rangle\,, \tag{7b}$$

$$P_2(\tau)=\frac{1}{N}\sum_{i=1}^{N}\tfrac{1}{2}\langle 3\cos^2[\theta_i(\tau)-\theta_i(0)]-1\rangle\,, \tag{7c}$$

where the angular bracket indicates a time average. $V_\theta(\tau)$ [Eq. (7a)] is the velocity autocorrelation function of this system which is related to the self-diffusion coefficient. $P_1(\tau)$ and $P_2(\tau)$ represent the first and second Legendre polynomials of the rotational dipole (i.e., the net change in torsional angle), which are related to dielectric dispersion, and NMR relaxation, respectively (for example). Note, that since all the beads are identical, we are averaging over all the beads.

Simulations were performed in the following way: Initial conditions were zero angular positions and velocities. Representative trajectories for the model systems behavior were generated by the Helfand method.[25] The time step was chosen such that a time average of the kinetic energy yielded the equipartition value of $NT/2$ (in dimensionless units). A time step $\delta t=0.1$ was found to be suitable for the parameters considered. Time averages were calculated in the following fashion: For some arbitrary quantity $F_i(t)$ the time average is given by

$$\langle F_i\rangle=\frac{1}{M}\sum_{l=1}^{M}F_i(l\delta t)\,, \tag{8}$$

where $F_i(l\delta t)$ is the quantity $F_i(t)$ evaluated at the time $t=l\delta t$ and M is the number of time steps of the simulation over which averaging was carried out. For instance, to calculate the average kinetic energy of the system, we would set $F_i(t)=\frac{1}{2}\dot\theta_i^2(t)$, perform the sum in Eq. (8), and then average over all the beads. Generally, simulations were run for 20 000 time steps during which time averages were performed.[26] Correlation functions were calculated as follows [again for an arbitrary quantity, $F_i(t)$];

$$\langle F_i(\tau)F_i(0)\rangle=\frac{1}{M}\sum_{l=1}^{M}F_i(l\delta t)\,F_i[(l+k)\delta t]\,, \tag{9}$$

where $F_i(t)$ is evaluated at $t=l\delta t$ and $t+\tau=(l+k)\delta t$, respectively. To evaluate Eq. (7a), e.g., $F_i(t)$ would be set equal to $\dot\theta_i(t)$. The values of the correlation functions were examined at 10 000 time steps and also at 20 000 time steps and were found to be essentially the same. Thus, these functions had achieved their steady-state values.

III. SIMULATION RESULTS

A. No twist: $\delta=0$

We first considered a system with only torsional coupling between the beads and no additional rotational potentials; i.e., the "no barrier" system. There are no twists introduced into the chain at this point ($\delta=0$). This system has been examined by several authors[14–16] and analytic solutions have been developed for various correlation functions in the case of overdamped friction constants. A comparison between simulation and theoretical results provided a further check on the efficacy of our simulation. Additionally, this system is the simplest one described by Eqs. (5) and (6) and hence is a natural starting point.

The analytic formulation of Schurr *et al.*[16] is most convenient for our purposes. They note that the set of Langevin equations describing the system of torsion-coupled beads are essentially identical to those of a circular, free-draining Rouse–Zimm model. They obtain the following correlation function (in our notation using dimensionless units):

$$\frac{1}{N}\sum_{i=1}^{N}\langle\exp\{ik[\theta_i(\tau)-\theta_i(0)]\}\rangle = \exp(-k^2T\tau/N\beta)\exp\left\{-\frac{k^2}{N}\sum_{i=1}^{N-1}d_i^2[1-\exp(-\tau/\tau_i)]\right\}, \tag{10}$$

where

$$\tau_i=\beta/4K\sin^2(\pi l/N)\,, \tag{11a}$$

$$d_i=T/4K\sin^2(\pi l/N)\,, \tag{11b}$$

and k is an integer $k=1, 2, \ldots$.

From Eq. (10), we can obtain $P_1(\tau)$ and $P_2(\tau)$. In Fig. 1, we have plotted $P_1(\tau)$ and $P_2(\tau)$, both as given by the analytical solution and by the simulation. The agreement between the theoretical and simulation results is seen to be quite good, both for $P_1(\tau)$ and $P_2(\tau)$. Note

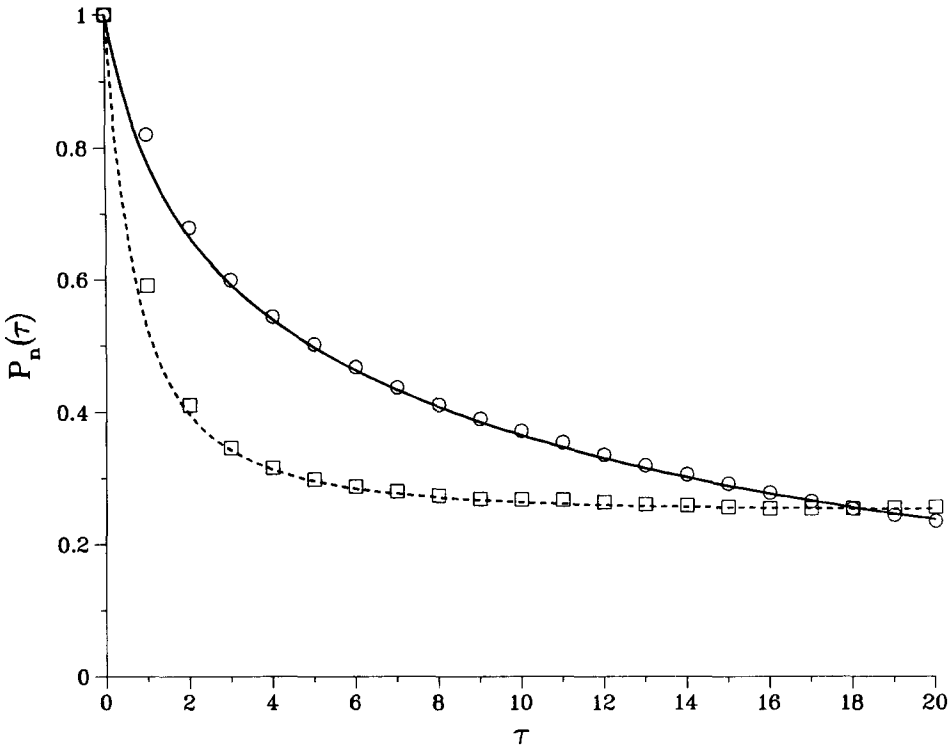

FIG. 1. Comparison of analytical and simulation results for $P_1(\tau)$ and $P_2(\tau)$. Solid and dashed lines are the analytical curves for P_1 and P_2, respectively. Circles and squares are the simulation results for P_1 and P_2, respectively.

that at short times, the simulation points are slightly above the corresponding analytical values. This difference is a result of the fact that the analytical calculation assumes an overdamped system and drops the inertial terms in the Langevin equations. The simulation, on the other hand, retains all the inertial terms. Thus, even though the system is overdamped (in the sense described in the previous section), the inertial character shows up through slightly stronger correlations at short times than is evident when these effects are neglected. The excellent agreement with theory displayed in Fig. 1 indicates that the simulation is working correctly. This gives us confidence to investigate variations of the model for which we do not have the corresponding analytical solutions.

We next considered the effect of additional, single-particle rotational potentials; i. e., $E_b \neq 0$. In Figs. 2 and

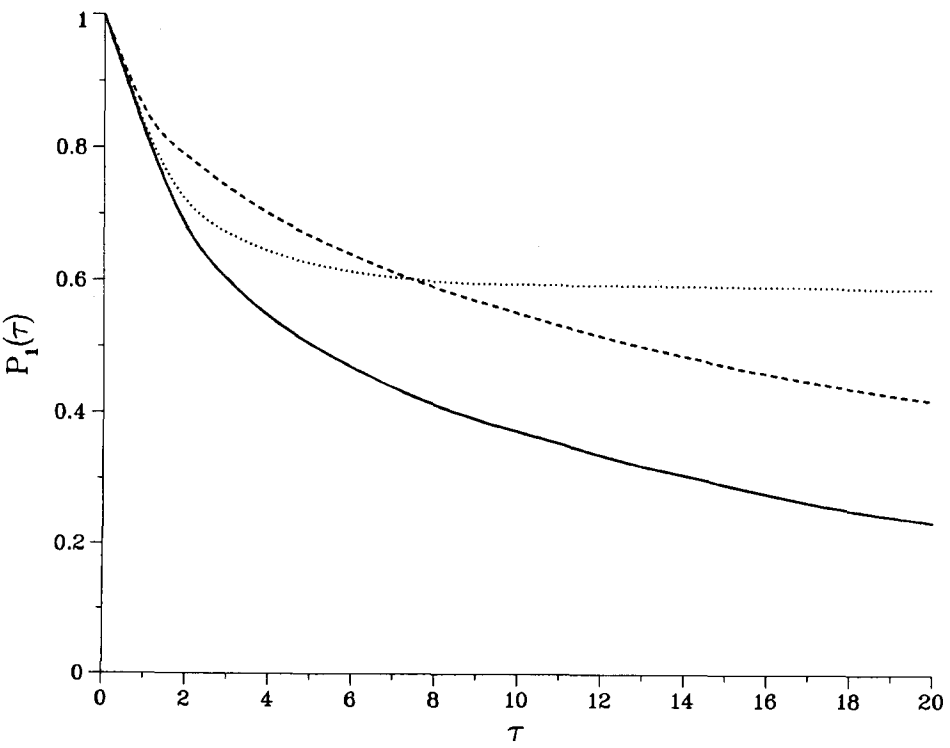

FIG. 2. P_1 vs τ for three model systems; the no barrier system (solid line), the onefold barrier system (dotted line), and the threefold barrier system (dashed line). The barrier height is $2T$ (dimensionless units) for the latter two systems.

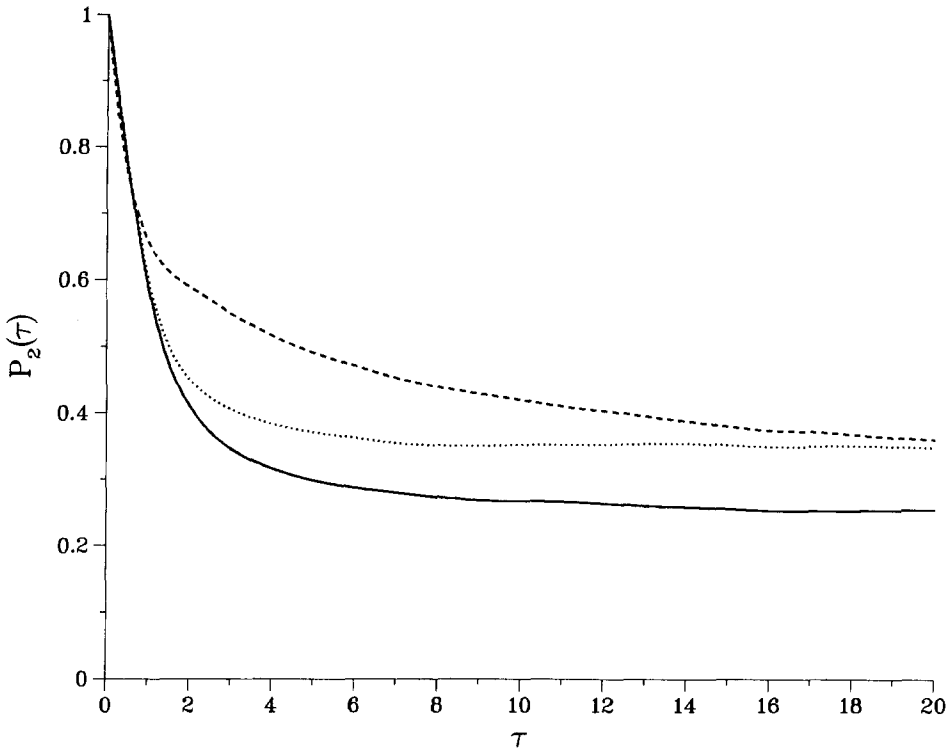

FIG. 3. P_2 vs τ for the three model systems described in Fig. 2.

3, we have plotted the $P_1(\tau)$ and $P_2(\tau)$ correlation functions, respectively, for the cases of no additional barriers, onefold barriers, and threefold barriers where $E_b = 2T$ for the barrier heights. In these figures, the various lines solid, dashed, and dotted are interpolated curves to the values of the correlation function as obtained by the simulations and denote the no barrier, one- and threefold barrier systems, respectively.

In Fig. 2 which depicts $P_1(\tau)$ vs τ, we see that the curves for the one- and threefold barrier systems lie above that of the no barrier system. This is not surprising as the rotational barriers act to confine the beads and thus the systems with barriers exhibit stronger correlations. What is of interest, however, is that the curves of the one- and threefold systems cross. This can be explained physically in the following manner. The onefold barriers are wider and less steep than those of their threefold counterparts, a consequence of the latter having more barriers per unit angular distance. Thus, the beads initially lose more correlation in the onefold case than in the threefold case because the threefold system constrains its beads more strongly. In other words, the beads have a shorter distance to go before a first collision with the barrier in the threefold system than in the onefold system. For longer times, however, the beads in the onefold case will feel the effects of their barriers and so the correlation does not continue to drop but instead levels off. The threefold system, on the other hand, has more states (or potential minima) in which to distribute the beads and hence this system shows a greater loss in correlation as time increases. Thus, the curve for the threefold system crosses that of the onefold case. We see this effect also occurring in Fig. 3 for the $P_2(\tau)$ correlation where the crossing has not quite occurred but can be extrapolated from the slopes of the curves. We should note that this crossing phenomena has also been observed by Cook and Livernese[18] in their simulations of slightly different model systems.

In Figs. 4 and 5, we again compare the $P_1(\tau)$ and $P_2(\tau)$ correlation functions for the same systems as those of Figs. 2 and 3 but with $E_b = 3T$, a more realistic barrier height for polymers. We see that the behavior here is qualitatively the same as that for the systems with $E_b = 2T$. The correlations are stronger here than the corresponding $2T$ barrier height systems because of the steeper barriers. Note that the crossing phenomena occurs at a slightly later time. Again, this is due to the steepness of the $3T$ barriers.

An interesting effect is seen in Fig. 5 which depicts the P_2 autocorrelation function. The curve for the threefold system shows a slight leveling off around $\tau = 1$. The beads have had their first collision with the barriers and are temporarily constrained. Thus, the correlation levels off. It then drops again because the beads begin diffusing over the barriers. This shows up most strongly in $3T$ barrier height systems because the steepness of the barriers can constrain the beads longer than in the $2T$ barrier system where the beads immediately begin diffusing over the barriers after their first collision. However, if one looks closely at the $2T$ systems, a slight indication of this leveling off can be seen for the threefold case. It should be noted that $\tau = 1$ is also where the first rebound effect is seen in the velocity autocorrelation function which will be presented below.

We now turn to examining how these correlation functions (and in addition, the velocity autocorrelation function) change when topological kinks are introduced into the model systems.

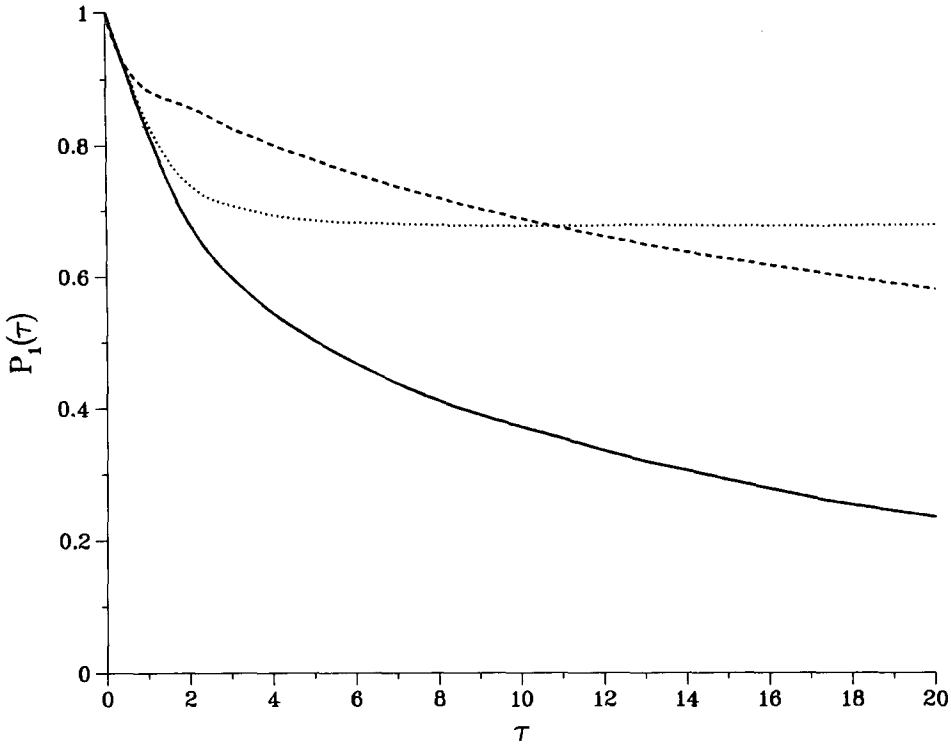

FIG. 4. P_1 vs τ for the three systems described in Fig. 2. Here, $E_b = 3T$.

B. Twists: $\delta \neq 0$

As described in Sec. II, we can introduce a topological kink or soliton into the system by making the parameter δ nonzero thereby placing a twist on the spring between the first and Nth beads. This causes the chain to maintain a phase difference of magnitude δ along the chain from θ_1 to θ_N. We wish to study how a nonzero δ affects the three correlation functions $P_1(\tau)$, $P_2(\tau)$, and $V_\theta(\tau)$.

However, before examining the correlation functions we shall look at the shape of the kink itself, that is how the twist is distributed along the chain. To this end, we did the following; a simulation of a particular sys-

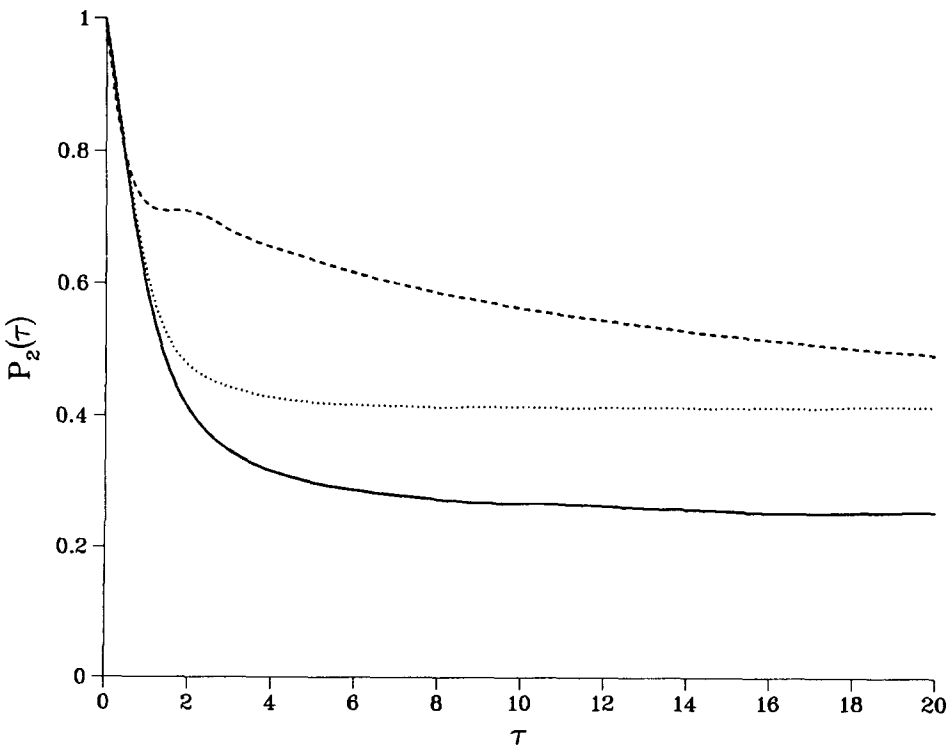

FIG. 5. P_2 vs τ for the three systems described in Fig. 2. $E_b = 3T$.

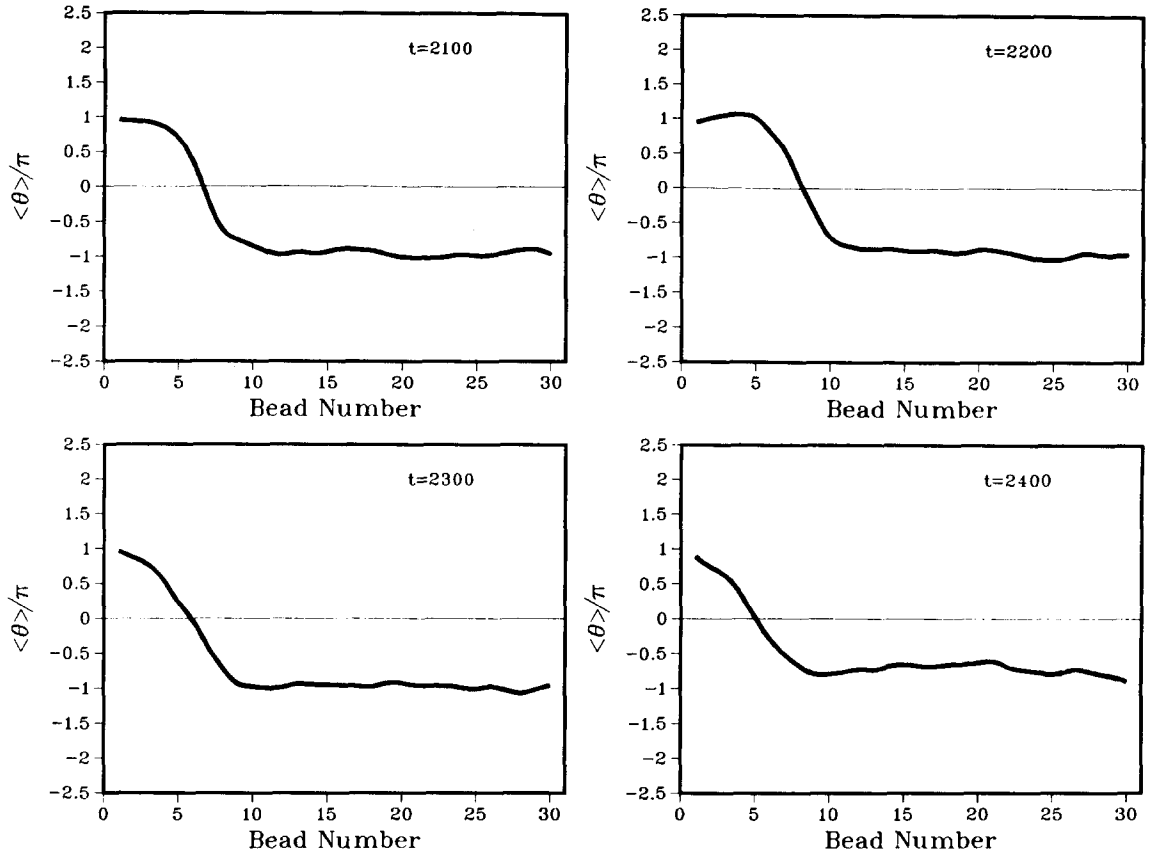

FIG. 6. Profile plot for the onefold barrier system ($E_b = 2T$) that contains a 2π twist. The average angular distance from a baseline midway between the average angular position of the first and Nth beads is plotted vs bead number.

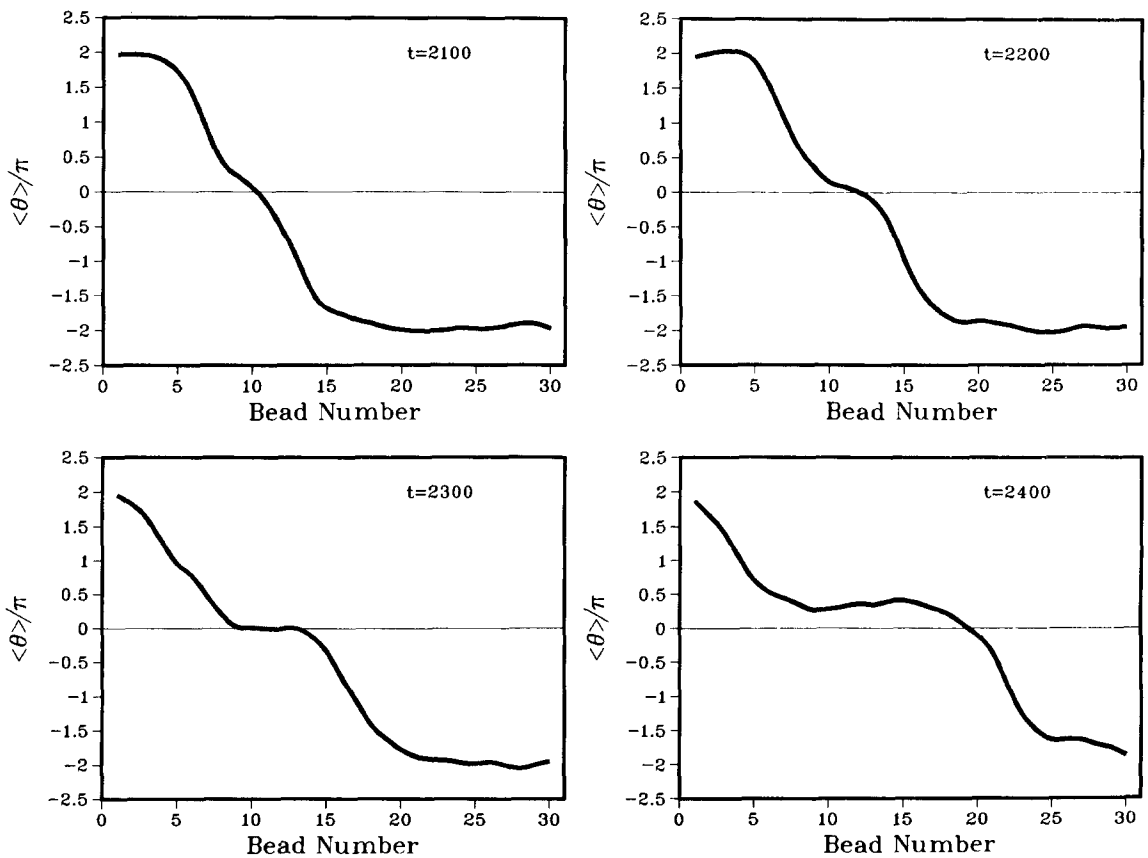

FIG. 7. Profile plot for the same system as Fig. 6 but with a 4π twist.

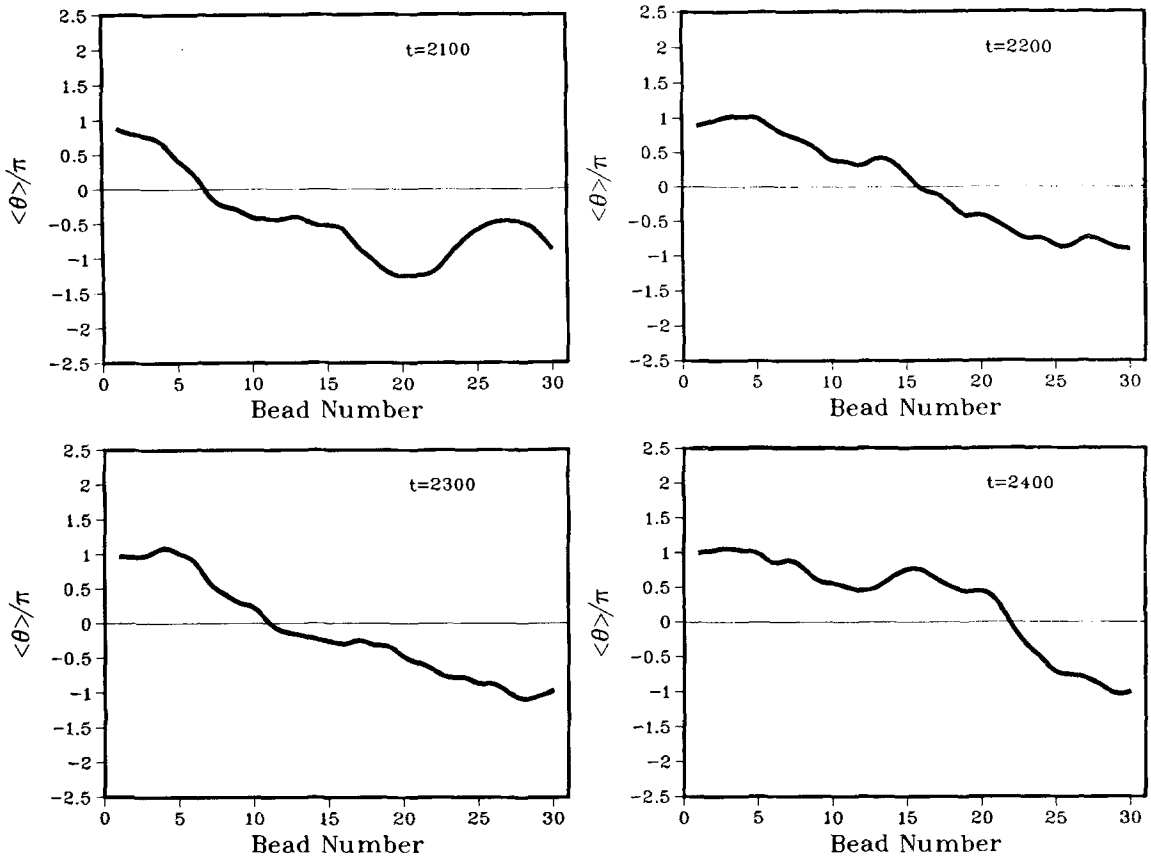

FIG. 8. Profile plot for the threefold barrier system ($E_b = 2T$) that contains a 2π twist.

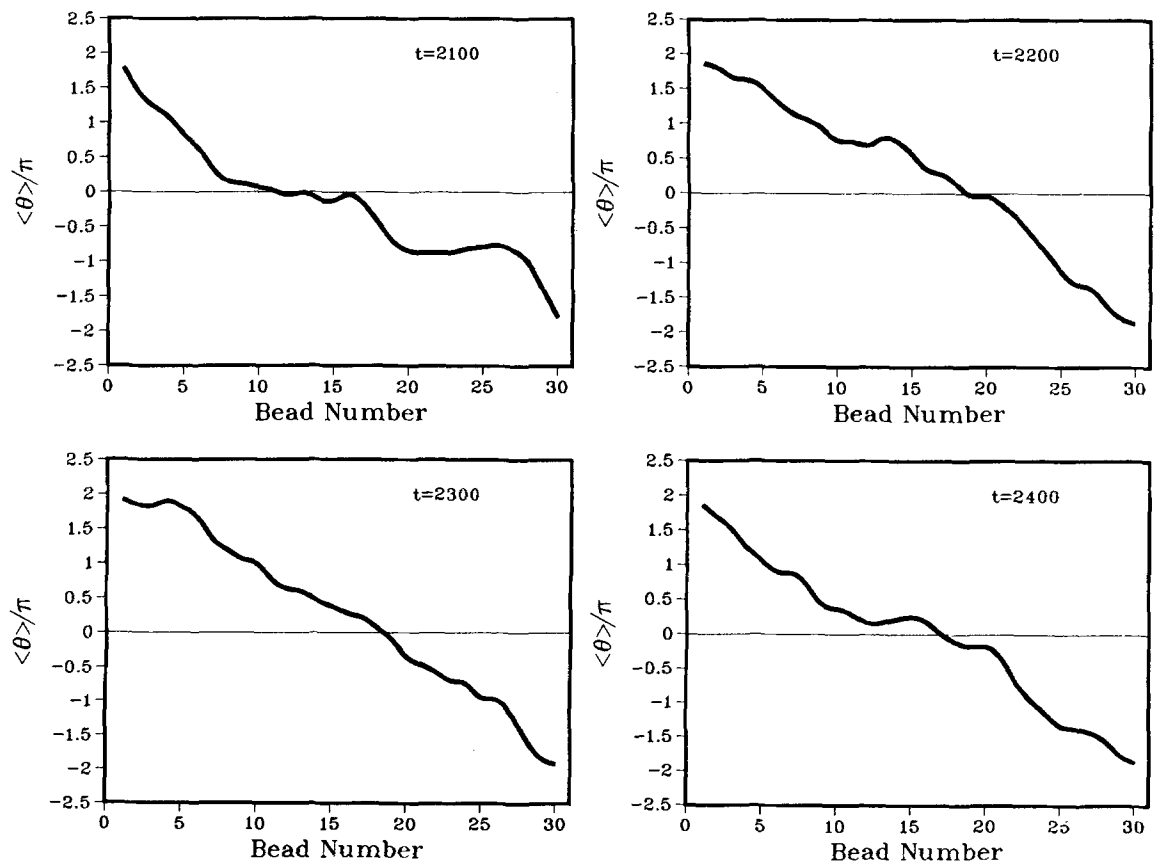

FIG. 9. Profile plot for the same system as Fig. 8 but with a 4π twist.

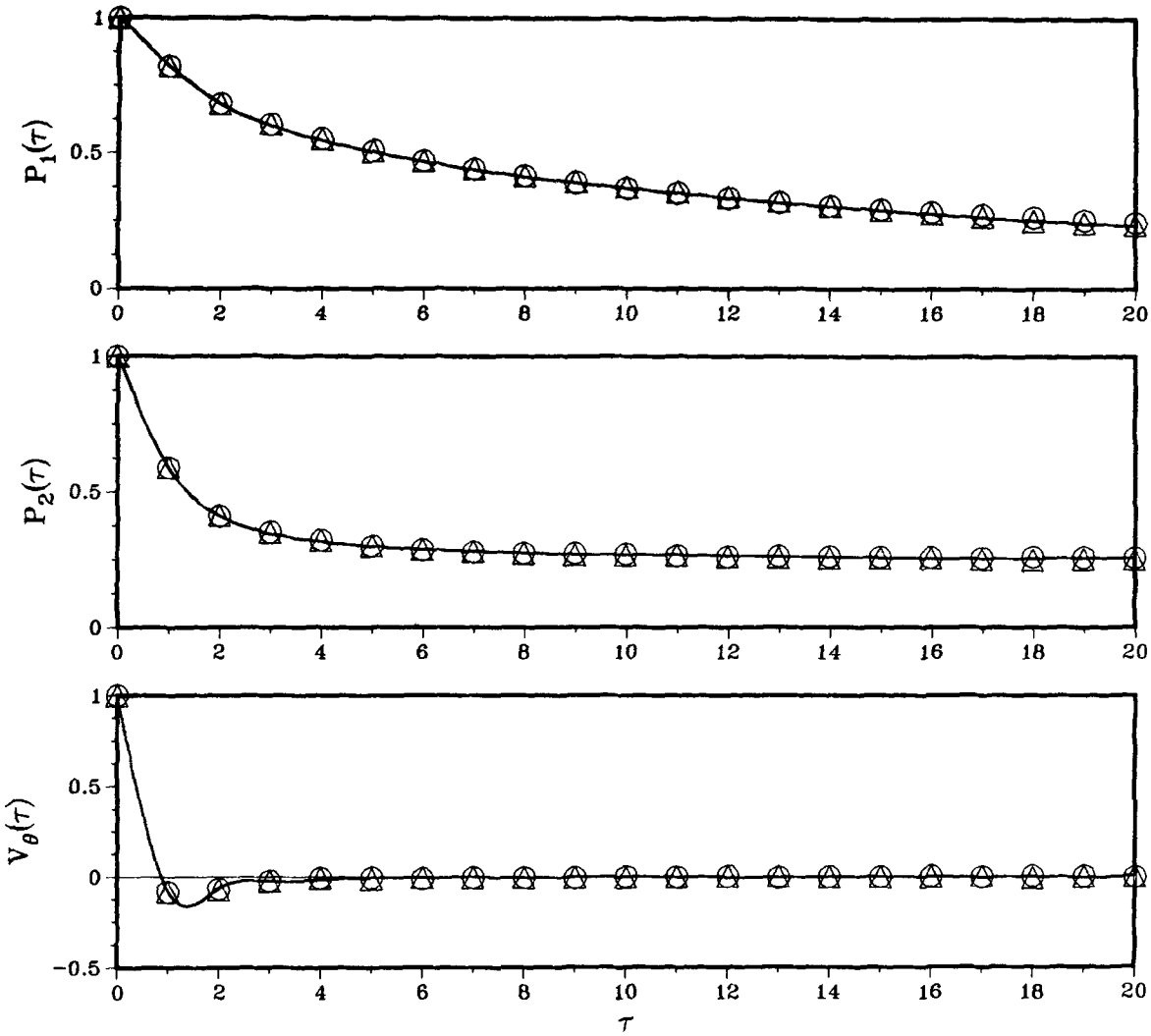

FIG. 10. Plots of the three autocorrelation functions P_1, P_2, and V_θ vs τ for the no barrier system, with no twists (solid lines), one twist (circles), and two twists (triangles).

tem was run for a length of time such that it was in equilibrium (typically, 20 000 time steps). The simulation was then continued and after the next 1000 time steps, a time average of the angular position of each bead was performed. These results were stored and the simulation continued. Averages were performed over the next 1000 time steps, the values stored, and so on. Thus, we had a series of "snapshots" of the kink profile. The choice of 1000 time steps for the averaging was dictated by the fact that for all the simulations performed, the time average of the kinetic energy of the system reached its steady state value in approximately 1000 time steps. Thus, it was felt that an average on this order of time would be long enough to average out the noise of the system and thus reduce scatter in a plot of the kink profile (i. e., angular position of each bead vs bead number), but not so long as to wash out the kink profile due to the diffusive nature of the kink itself. Note that this is a "measurement" specific to the soliton.

Figure 6 shows the kink profile at four different times (increasing time goes from top left to right, then bottom left to right) for the onefold barrier system ($E_b = 2T$) with a 2π twist. (It is pointless to present the no-barrier case, since as expected the twist quickly delocalizes over the whole chain.) To eliminate any overall rotation of the chain, we have plotted the kink profile as the average angular distance of each bead from a baseline midway between the average angular position of the first and Nth beads. In these profile plots we see that the kink is fairly localized and that its diffusive motion is rather slow.

In Fig. 7, we see profile plots for the same onefold barrier system but now containing a 4π twist. Here, we see something rather interesting. First, consider the first kink profile plot at time $t = 2100$. There, we see a phase difference of 4π along the chain as we should. However, note that there is a very slight leveling off around the baseline. As we look at the subsequent profile plots we see that this leveling off widens. What is happening is that the 4π twist separates into two 2π twists, i. e., instead of one kink, we have two. This is not surprising, since from the viewpoint of energetics, this is an easier way for the chain to support a 4π phase difference. And, in general, a phase δ will appear on the

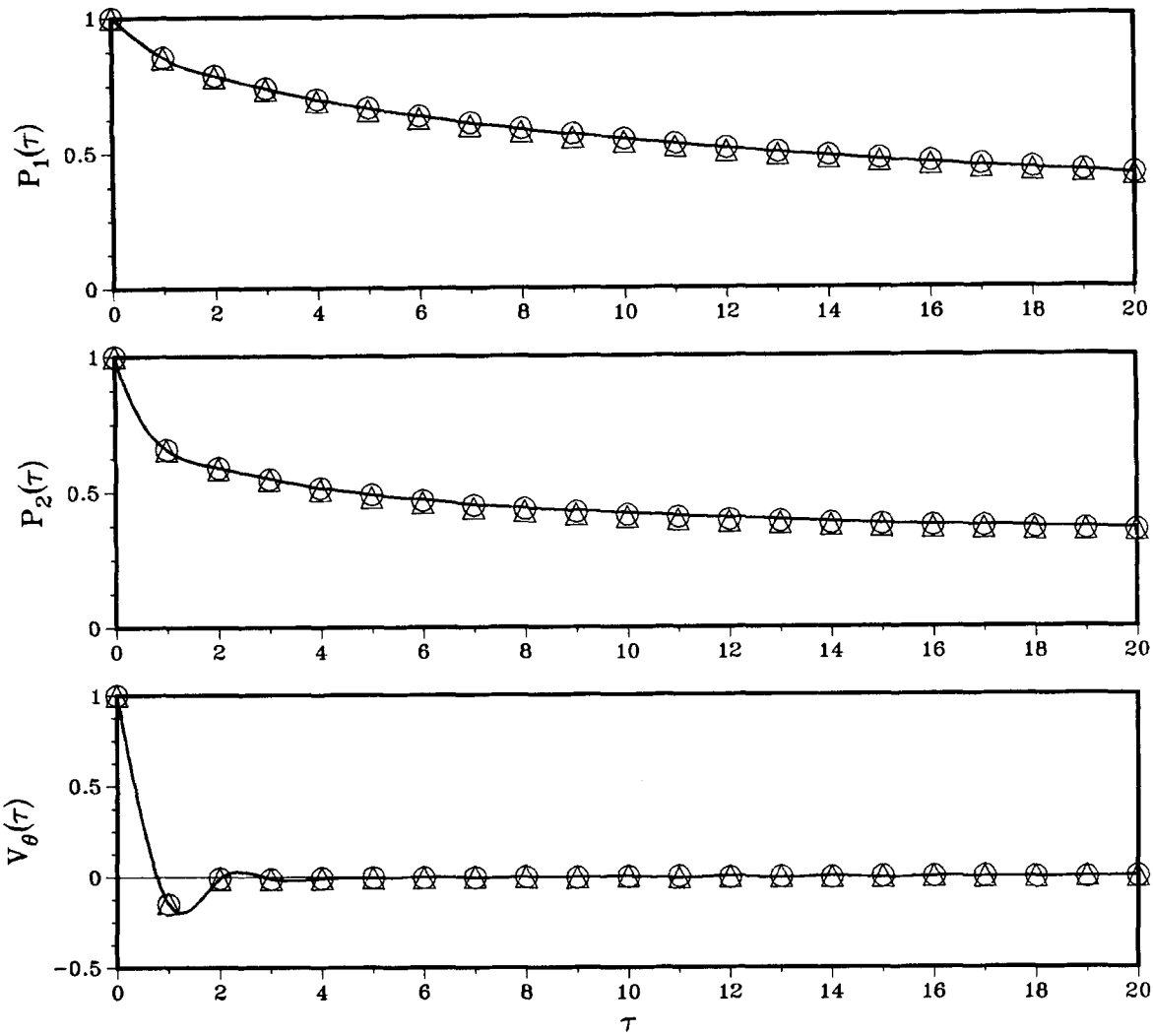

FIG. 11. P_1, P_2 and V_θ vs τ for the threefold barrier system ($E_b = 2T$) with no twists (solid lines), one twist (circles), and two twists (triangles).

chain as $\delta/2\pi$ kinks for the one barrier system.[19] Because of thermal fluctuations, and the reentrant boundary conditions, these two kinks will alternately combine into one kink and separate back into two kinks.

Figures 8 and 9 show kink profiles for the threefold barrier system ($E_b = 2T$) with 2π and 4π twists, respectively. The profiles are plotted in the same fashion as described in Fig. 6. In Fig. 8, we see that the motion of the single kink is much the same as that of the onefold barrier system but we note that the kink is spread out over a greater number of beads. This is due to the greater number of potential minima per angular distance in the threefold barrier system. Figure 9 shows this same system but with a 4π twist. In this example we see the system initially as two kinks which in the second and third time frames have diffused together and combined into a single 4π kink. In the fourth time frame the two kinks have again started to separate. Thus, in these four time frames we are looking at a soliton–soliton scattering event. These kinks are also spread out over a greater region than their onefold barrier counterparts. Since we see that in general the 4π twist splits into two 2π twists we shall refer to the 2π and 4π twists as single and double (or one and two) twists or kinks, respectively.

Now that we have developed a picture of the kinks we are in a position to obtain the correlation functions of the systems with kinks. Let us again begin with the case where there are no additional rotational barriers. In Fig. 10, we present three plots of P_1, P_2, and V_θ vs τ, respectively, for the cases where $\delta = 0$, 2π, and 4π. Thus, we are comparing similar systems where the chains are constrained to support no twists, one twist, and two twists. The solid lines in all three plots in Fig. 10 represent interpolated curves to the no twist simulation results; the circles and triangles are respectively the values for the one and two twist simulation results. As can be seen from these plots in Fig. 10, the presence of kinks in the no barrier system has a negligible effect on these three correlation functions. Physically, this is not surprising. The torsion-coupled bead system is essentially a system of harmonic oscillators. The introduction of the twist (or twists) does not change this fact. Because there are no rotational bar-

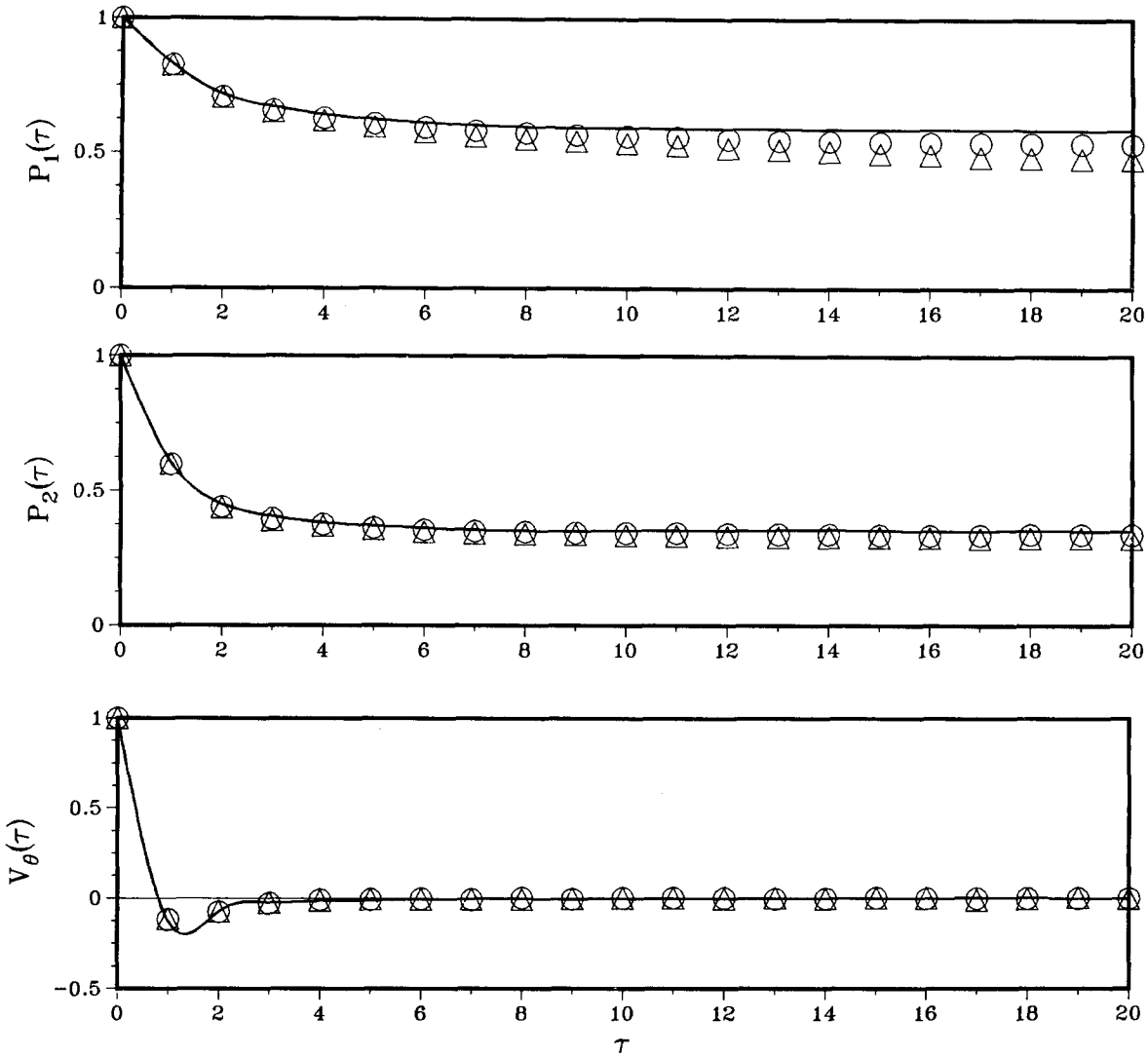

FIG. 12. P_1, P_2, and V_θ vs τ for the onefold barrier system ($E_b = 2T$) with no twists (solid lines), one twist (circles) and two twists (triangles).

riers, the twist can quickly delocalize over the entire chain thus creating a set of harmonic oscillators which are shifted by a linear term in the Hamiltonian. A simple coordinate transformation can return one to the standard harmonic oscillator equations. We then have a set of rescaled harmonic oscillators. Thus, one should not expect, and one does not see, any major differences in the correlation functions when comparing the kinked, no barrier systems with their nonkinked counterparts.

Next, we consider the kinked and nonkinked versions of the threefold barrier system (for $E_b = 2T$). The $P_1(\tau)$, $P_2(\tau)$, and $V_\theta(\tau)$ correlation functions are plotted in Fig. 11 in exactly the same fashion as described for Fig. 10. Again, we see that the introduction of twists has a negligible effect on these three correlation functions. V_θ appears to be essentially transparent to the twists. P_1 and P_2 show almost no deviation for the single twist (1.2% at max for P_1, 2.0% for P_2), and a slight deviation for two twists (2.0% at max for P_1, 3.7% for P_2). Note that although the deviations are extremely small, the twists appear to lower the correlations (excepting V_θ) and two twists have a larger effect than one twist.

In Fig. 12, we have plotted the three correlation functions for the kinked and nonkinked onefold barrier systems. Here we finally see a noticeable and systematic difference in P_1 and P_2 because of the twists. However, the velocity autocorrelation function is still unaffected by the twists. For P_1 and P_2 we definitely see a lowering of the correlations and the magnitude of the change increases with the number of twists. We must point out though, that this change is still rather small. For the single twist, P_1 shows a maximum deviation of 8.8% and that of P_2 is 5.2%. For two twists the maximum deviations are 18.3% for P_1 and 7.7% for P_2.

In Fig. 13, we again compare kinked and nonkinked versions of the threefold barrier systems but with the barrier height $E_b = 3T$. Here we only plot the double twist since that appears to produce the most difference from a no twist situation (when an effect is seen at all). The velocity autocorrelation function is again transparent to a twist. P_1 and P_2 show only slight deviations

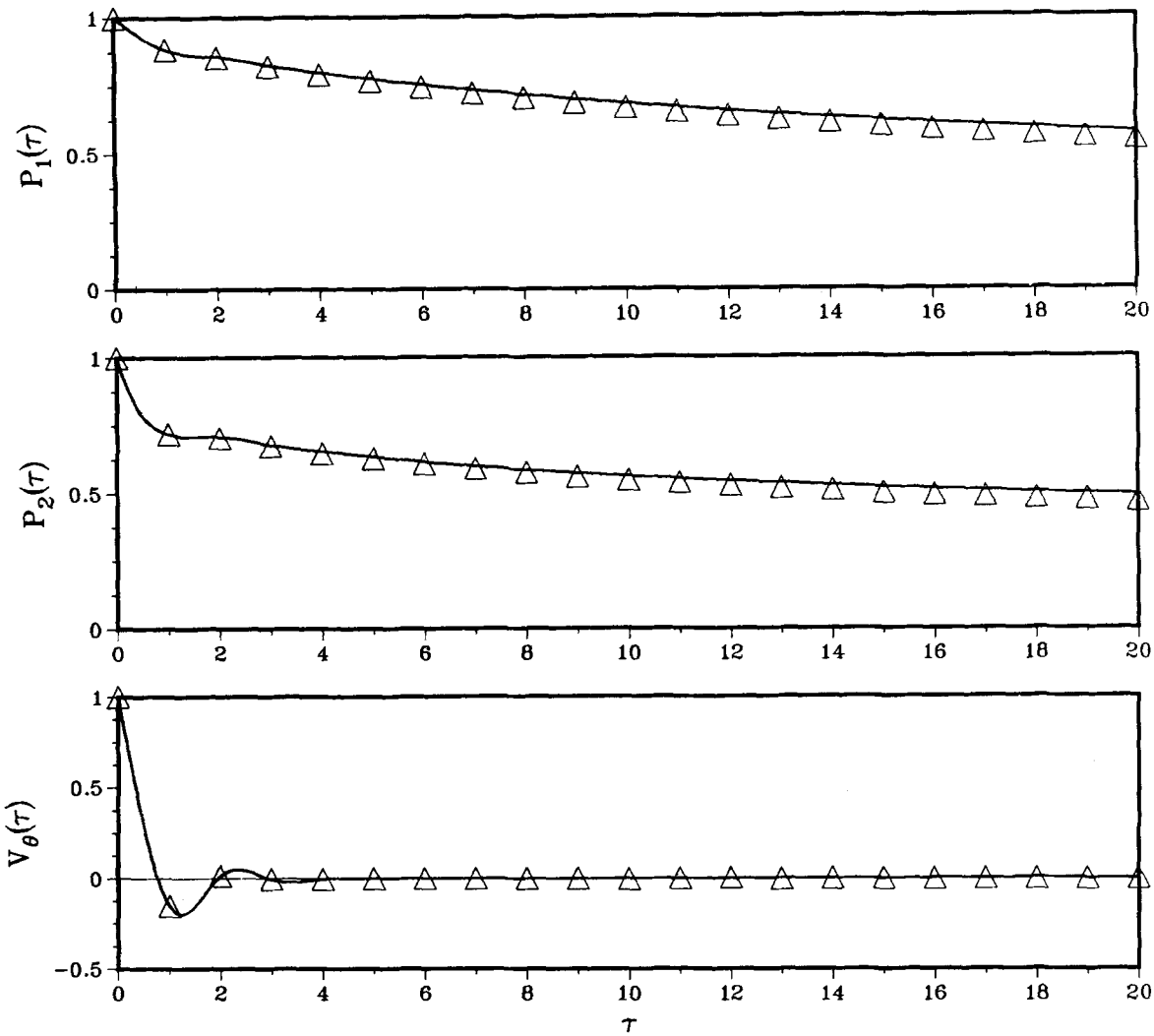

FIG. 13. P_1, P_2, and V_θ vs τ for the threefold barrier system ($E_b = 3T$) with no twists (solid lines) and two twists (triangles).

(4.9% for P_1 at max, 4.8% for P_2).

Figure 14 compares the kinked (two twists) and non-kinked onefold barrier system with $E_b = 3T$. No effect is seen in V_θ. P_1 and P_2 show deviations comparable to their $E_b = 2T$ counterparts (16.9% for P_1 and 9.6% for P_2).

IV. DISCUSSION

We have utilized the technique of Brownian dynamics to investigate the effects of kinks or solitons on various torsional oscillator models. The models we studied were: (1) nearest-neighbor torsion-coupled beads (the no-barrier system); (2) torsion-coupled beads with additional threefold rotational potentials (the threefold barrier system); and (3) torsion-coupled beads with additional onefold rotational potentials (the onefold barrier system). These models are of interest because of their application to torsional motions in polymers and in the torsional dynamics of DNA. The last model, the sine-Gordon chain, is of interest in many areas beyond that of polymers. Since reentrant boundary conditions were used for each system, topological kinks or solitons could be introduced into the system by placing a twist (or twists) on the spring connecting the first and Nth beads which forces the chain to support a phase difference along the chain equal to the magnitude of the twist.

Our primary interest lay in determining the effect of topological kinks on typical experimental quantities. To this end, we performed the following computer experiments. We simulated the behavior of each of the above systems both with and without topological solitons (i.e., systems with twists and systems without twists). In the process, we measured three autocorrelation functions; the velocity autocorrelation function $[V_\theta(\tau)]$ and the first and second Legendre polynomials $[P_1(\tau), P_2(\tau)]$ of the rotational dipole (the net change in torsional angle). These correlation functions are related to various experimentally measured quantities including light scattering, NMR relaxation times, fluorescence depolarization, and dielectric and mechanical relaxation. The advantage of considering topological kinks is that, unlike the dynamic solitons which appear or disappear as soliton–antisoliton pairs due to thermal fluctuations, the

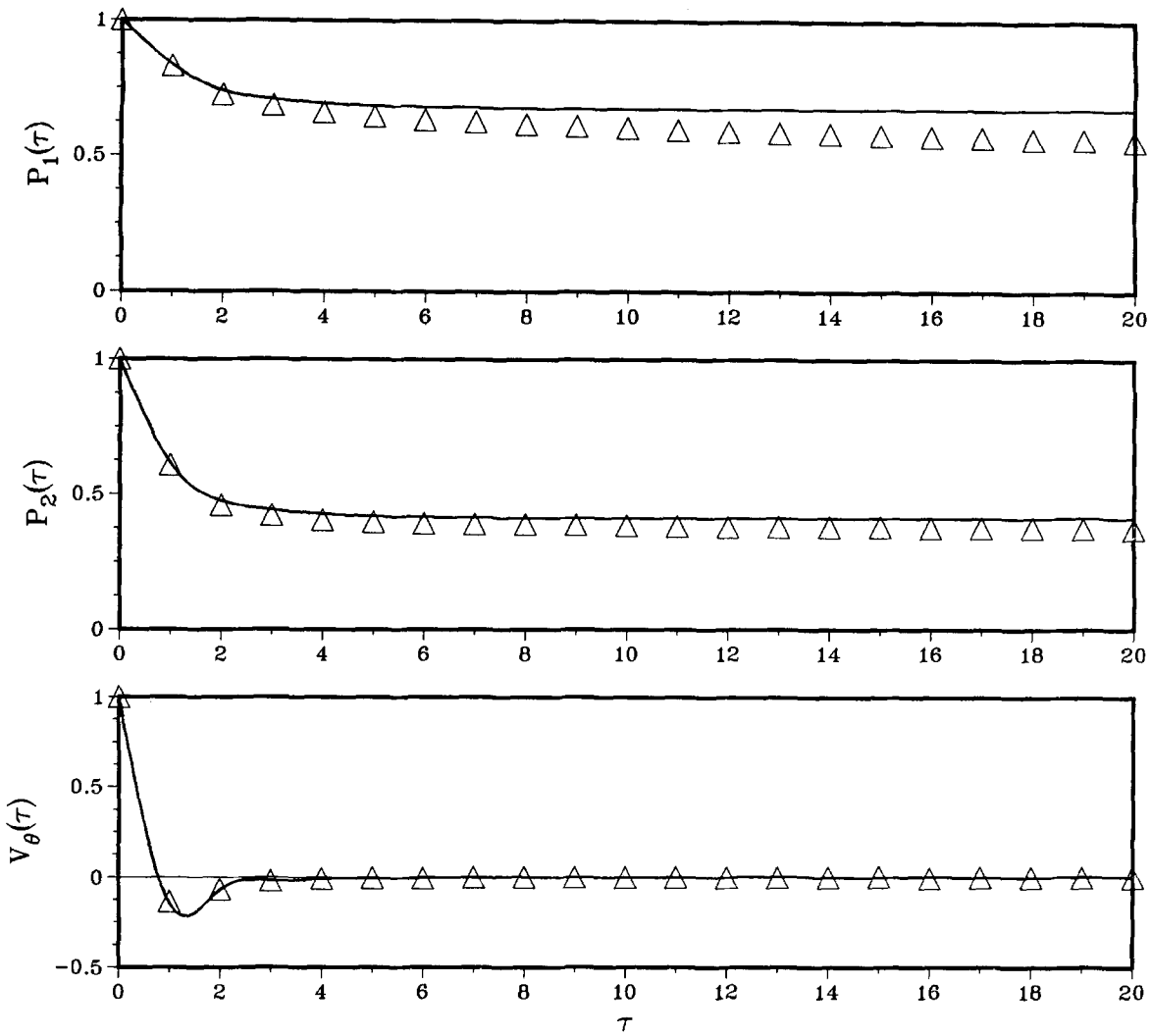

FIG. 14. P_1, P_2, and V_θ vs τ for the onefold barrier system ($E_b = 3T$) with no twists (solid lines) and two twists (triangles).

topological ones remain in the system and we can directly control their absence or presence.

The results of the comparison of the P_1, P_2, and V_θ correlation functions of the kinked model systems with their nonkinked counterparts can be summarized briefly as follows:

(1) The velocity autocorrelation function, V_θ appears to be totally insensitive to the presence of kinks for all of the model systems studied.

(2) For the no barrier system P_1 and P_2 are also insensitive to the kinks. This is due to the fact that the kink delocalizes along the entire chain, thus producing a set of shifted harmonic oscillators which behaves no differently than the nonkinked system.

(3) For the threefold barrier system with $E_b = 2T$, a single twist produces almost no discernible difference from the nonkinked system for both P_1 and P_2. Two twists show a slight deviation. For $E_b = 3T$, we only considered two twists. There, P_1 and P_2 were lowered by a small amount (less than 5% at maximum).

(4) For the onefold barrier system with $E_b = 2T$, a single twist produces almost no effect on P_2 but does produce a small lowering of P_1 from its nonkinked counterpart. Two twists deviate slightly more than one twist. This effect, though is less than 18.3% for P_1 and 7.7% for P_2. For $E_b = 3T$, we again only considered a double twist. There, the effects were similar to the $E_b = 2T$ case.

In conclusion, for the model systems studied and the parameters used, the presence of toplogical kinks or solitons does not produce a major change in typically measured autocorrelation functions. In particular, the sine-Gordon chain (onefold barrier) was the only system to show any significant effect due to the presence of solitons. However, this effect was only sizeable for the P_1 correlation function and even here the maximum change was less than 20%. In addition this maximum change was seen in the two kink system and it should be realized that two kinks per 30 units (beads) is an unrealistically high density of solitons for a physical system. For the three barrier case which is more relevant to polymeric systems (and also for the no-barrier case) there is essentially no change in the correlation functions on the addition of even this unrealistically high soliton density.

The simulation suggests that such nonspecific probes as the ones we examined are unlikely candidates to see the effects of solitons. If one wants to observe the solitons in a physical system, experimental probes should be used which are specific to the types of solitons of interest, or to the specific changes in the eigenvalue spectrum (i.e., the new eigenvalues) introduced by the solitons.

ACKNOWLEDGMENTS

This study was supported in part by the National Science Foundation (Polymer Program), Grant #DMR-8007025. Acknowledgment is also made to the Donors of the Petroleum Research Fund, administered by the American Chemical Society, for partial support of this research. The computations reported on here were carried out on the Washington University Computing Facility IBM family of computers (primarily the IBM 370/158 systems).

[1]J. Frenkel and T. Kontorova, J. Phys. (Moscow) 1, 137 (1939).
[2]D. Perchak and J. H. Weiner, Phys. Rev. B 22, 2683 (1980).
[3]U. Enz. Helv. Phys. Acta 37, 245 (1964).
[4]W. P. Su, J. R. Schrieffer, and A. J. Heeger, Phys. Rev. Lett. 42, 1698 (1978), and Phys. Rev. B 22, 2099 (1980).
[5]S. Kivelson and D. E. Helm, Phys. Rev. B 26, 4278 (1982).
[6]J. L. Skinner and P. G. Wolynes, J. Chem. Phys. 73, 4022 (1980).
[7]M. L. Mansfield, Chem. Phys. Lett. 69, 383 (1980).
[8]J. Goldstone and R. Jackiw, Phys. Rev. D 11, 1486 (1975).
[9]For reviews see A. C. Scott, F. Y. F. Chu, and D. W. McLaughlin, Proc. IEEE. 61, 1443 (1973); A. Barone, F. Exposito, C. J. Magee, and A. C. Scott, Riv. Nuovo Cimento 1, 227 (1971).
[10]E. M. Simon and B. H. Zimm, J. Stat. Phys. 1, 41 (1969).
[11]M. Fixman, J. Chem. Phys. 69, 1527 (1978), and following article.
[12]E. Helfand, J. Chem. Phys. 69, 1010 (1978).
[13]J. H. Weiner and M. R. Pear, Macromolecules 10, 317 (1977).
[14]D. K. Carpenter and J. Skolnick, Macromolecules 14, 1284 (1981).
[15]J. E. Shore and R. Zwanzig, J. Chem. Phys. 63, 5445 (1975).
[16]S. A. Allison and J. M. Schurr, Chem. Phys. 41, 35 (1979); S. C. Lin and J. M. Schurr, Biopolymers 17, 425 (1978).
[17]M. D. Barkley and B. H. Zimm, J. Chem. Phys. 70, 2991 (1978).
[18]R. Cook and L. L. Livernese, preprint.
[19]R. A. Guyer and M. D. Miller, Phys. Rev. A 17, 1205 (1978); 17, 1774 (1978).
[20]T. Schneider and E. Stoll, Phys. Rev. Lett. 41, 1429 (1978), and E. Stoll, T. Schneider, and A. R. Bishop, Phys. Rev. Lett. 42, 937 (1979).
[21]M. Büttiker and R. Landauer, Phys. Rev. Lett. 43, 1453 (1979).
[22]N. Gupta and B. Sutherland, Phys. Rev. A 14, 1790 (1976).
[23]J. F. Currie, J. A. Krumhansl, A. R. Bishop, and S. E. Trullinger, Phys. Rev. B 22, 477 (1980).
[24]M. B. Fogel, S. E. Trullinger, A. R. Bishop, and J. A. Krumhansl, Phys. Rev. Lett. 36, 1411 (1976).
[25]E. Helfand, Bell Syst. Tech. J. 58, 2289 (1979).
[26]For the systems with barrier heights $E_b = 3T$ it was necessary to run the simulations for 40 000 time steps.